PHILOSOPHICAL TRANSACTIONS OF THE ROYAL SOCIETY A MATHEMATICAL, PHYSICAL & ENGINEERING SCIENCES

The Control of Ductility on the Deformation of Pebbles and Conglomerates [and Discussion]

N. C. Gay, R. E. P. Fripp, B. A. Bilby and M. L. Kolbuszewski

Phil. Trans. R. Soc. Lond. A 1976 **283**, 109-128
doi: 10.1098/rsta.1976.0072

Phil. Trans. R. Soc. Lond. A. **283**, 109–128 (1976) [109]
Printed in Great Britain

The control of ductility on the deformation of pebbles and conglomerates

By N. C. Gay
Bernard Price Institute of Geophysical Research, University of the Witwatersrand, Johannesburg, South Africa

and R. E. P. Fripp
Department of Geology, University of the Witwatersrand, Johannesburg, South Africa

[Plates 4 and 5]

Pebbles are commonly used parameters for the determination of finite strain in deformed rocks. In high grade metamorphic environments, rocks probably behave as viscous fluids and a theory exists which relates the deformation experienced by a pebble to that of the host rocks. However, some deformed conglomerates are found in low grade metamorphic rocks where the assumption of viscous behaviour is unrealistic.

The deformation of artificial conglomerates made of geological materials, at room temperature and varying confining pressure is described. In these experiments, pebbles deform by cataclasis at surprisingly low applied loads and large finite strains are achieved. The amount of deformation experienced by pebbles of different rock types depends mainly on their yield strengths and ductility contrasts with respect to the matrix. A theoretical analysis assuming that pebble and matrix behave as work-hardening Bingham materials during deformation relates the strain experienced by a pebble to that of the host rock.

The results suggest that significant pebble deformation can occur during gravitational loading of sediments. An attempt is made to verify this idea by analysing the shape of pebbles in conglomerates of the Upper Witwatersrand System. At some sites the pebbles appear to have deformed during gravitational compaction while at others a tectonic deformation has been superimposed upon the pre-tectonic strain.

Introduction

Pebbles in deformed rocks provide important deformation on the amount of deformation experienced by rocks and on the rheological condition of rocks during deformation. Their use as parameters of finite strain is now well established and there exist reliable geometric techniques for allowing for the initial shape and orientation of the pebbles in deducing the finite strains (Ramsay 1967, pp. 202–221; Dunnet & Siddans 1971). However, to relate this pebble finite strain to that experienced by the whole rock requires some assumption on the rheological condition of the rock during deformation and Gay (1968) developed a theory to carry out this correlation, assuming that during deformation, the pebbles and host rock behaved as viscous fluids. Then, the factor controlling the relative amounts of deformation experienced by the individual pebbles and rock respectively is dependent on the ratio of the coefficients of viscosity of these components. The larger this ratio, i.e. the more viscous the pebble is compared to the whole rock, the less deformation it experiences. If the viscosity ratio exceeds 10, very large finite strains are required to cause significant changes in pebble shape.

The condition under which rocks behave as viscous fluids can be determined from the

published experimental work on the pseudoviscous flow of rock. This type of flow takes place while the rock is in a solid condition but has an equivalent viscosity which remains constant during specific deformation conditions and which changes with the shear stress and rate of strain; i.e. the rock is not a Newtonian fluid but approximates to one under the given conditions. Increases in temperature and stress difference cause a nonlinear decrease in this coefficient of viscosity; increasing confining pressure may increase the coefficient. The limited experimental data available (see, for example, Handin 1966; Heard 1976) suggest that temperatures of at least 400–500 °C (approximately half the melting temperature of the rock) and confining pressures of 300–400 MPa are required for rocks to deform by pseudoviscous flow at reasonable geological strain rates. The onset of viscous flow would also be enhanced by the presence of water to promote hydrolytic weakening.

These P, T conditions mean that conglomerates and other rocks containing pebbles must experience metamorphic conditions at least equivalent to greenschist facies (cf. Robertson 1972, p. 637) before the assumption of viscous behaviour during their deformation is valid. Many deformed conglomerates described by previous workers (e.g. Flinn 1956; Oftedahl 1947; Hossack 1968; Hasan & Sakar 1967; Gay 1969; Mukhophadhyay & Bhattacharya 1969) do show evidence of having experienced at least low grade regional metamorphism. This evidence includes the development of a schistosity and lineation associated with an episode of folding, mineralogical changes such as the alteration of feldspar and the formation of sericite, and the development of preferred orientations of quartz optic axes. In these examples, the assumption of viscous behaviour of the rocks during deformation may be valid, but conglomerates in which apparently deformed pebbles are found but which do not appear to be significantly metamorphosed may also exist. For example, in the Barberton Mountain Land, Transvaal, South Africa, conglomerates of the Moodies Group have been deformed during several episodes of folding (cf. Gay 1969; Anhaeusser 1974). Locally, some of the conglomerate outcrops have been metamorphosed to albite-epidote-hornfels grade (T = 500 °C, P = 200 MPa; Winkler 1967, p. 70) and others to upper greenschist grade, but there are regions, where no foliation is developed in the rocks and the P, T conditions are unlikely to have been sufficiently large to permit pebble deformation by viscous flow.

Occasionally, some pebbles in slightly metamorphosed conglomerates appear to have deformed by viscous flow whereas others have not, depending on the composition of the pebble. For example, figure 1*a* depicts an extremely attenuated chert pebble, the tail of which is distorted around a slightly deformed granite pebble; no cleavage is visible in the quartzite matrix. Similarly, in figure 1*b*, weak limestone pebbles (L) are extremely deformed while other, more competent pebbles are much less deformed and are cut by extension cracks.

In this paper, some recent experimental work by Gay & Jaeger (1975) on the deformation of artificial conglomerates, in which large finite strains are achieved by cataclastic flow is discussed; the experimental conditions are such as to preclude viscous flow. The term *ductility* is used intsead of the more precise 'viscosity' to describe the rheological condition of the deforming materials and also the condition of naturally deformed pebbles, which have obviously not been in a viscous state. Note that ductility is approximately equivalent to the reciprocal of viscosity; the more ductile a material is, the less viscous it is. In order to facilitate comparison between the ductility contrasts reported in this paper and viscosity contrasts reported elsewhere, the ratios of the ductility of the matrix to that of the pebble are used.

PHILOSOPHICAL TRANSACTIONS OF THE ROYAL SOCIETY A MATHEMATICAL, PHYSICAL & ENGINEERING SCIENCES

The results of the experiments suggest that significant deformation may take place at pressures comparable to those accompanying diagenesis of sediments ($T \leqslant 200$ °C, $P \leqslant 200$–300 MPa). Also described is the variation in strain in conglomerates near the top of the Upper Witwatersrand system as deduced from pebble shapes at localities on the northern edge of the Witwatersrand basin and around the Vredefort dome; these strain results support the experimental observations.

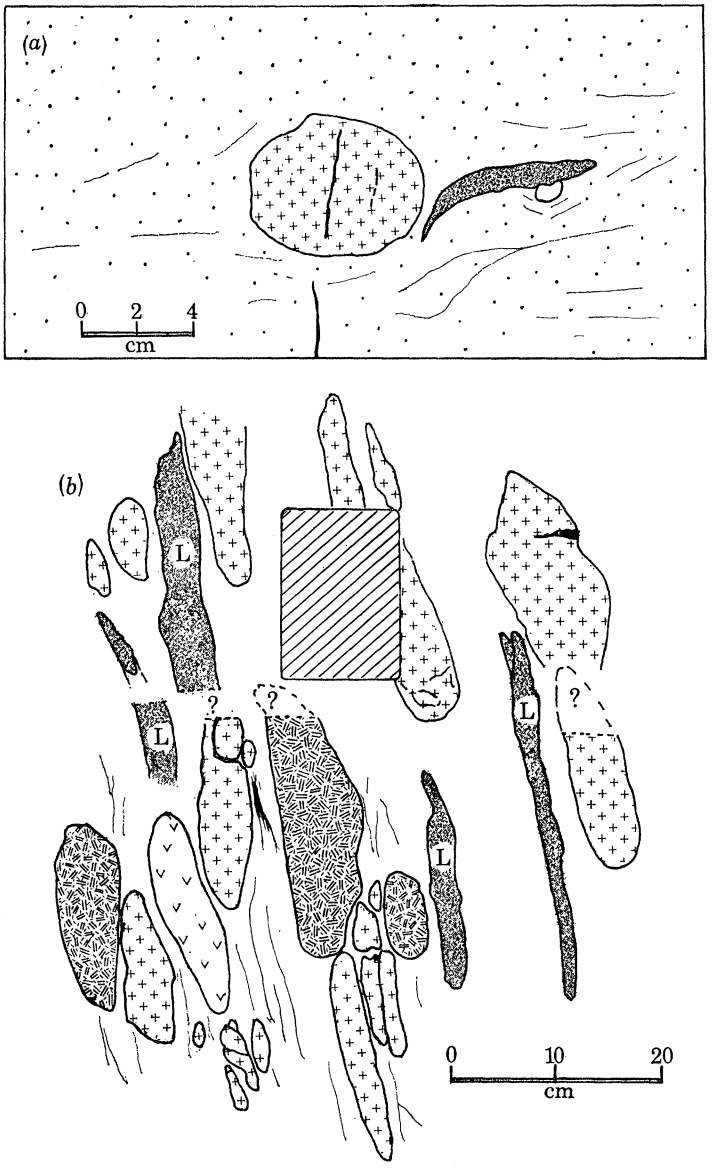

FIGURE 1. (*a*) Deformed chert and granite pebbles in the Moodies basal conglomerate, Eureka Siding, Barberton Mountain Land, South Africa. (*b*) Deformed limestone (L), quartzite, chert and acid volcanic pebbles in a conglomerate exposed along the Abercrombie River, New South Wales, Australia. (Sketched from photographs.)

PHILOSOPHICAL TRANSACTIONS OF THE ROYAL SOCIETY A MATHEMATICAL, PHYSICAL & ENGINEERING SCIENCES

Experimental work

(a) *Method*

Gay & Jaeger (1975) have described the deformation of artificial pebbles of rock set in a granular matrix during uniaxial compression of the pebble-matrix sample. The experimental technique involved placing a layer of crushed matrix in a thick-walled rubber jacket, then positioning the pebble (a sphere or 1:1 cylinder of rock 7 mm in diameter) in the centre of the matrix and covering it with another layer of matrix. The composite sample, usually of dimensions 50 mm diameter by 25 mm high, was placed in a compression testing machine and deformed under uniaxial loads ranging from 0.2 to 4.5 MN, which were applied at a fast, controlled rate. The matrix material was normally crushed Wombeyan marble but crushed adamellite and a marble-salt mixture were also used. Pebbles were prepared from sandstone, shale, Carrara marble, Solenhofen limestone, oolitic limestone, trachyte and quartzite. During the initial stages of loading considerable radial flow of the matrix occurs but, in addition, a layer of interlocked grains builds up on each platen which eventually forms a coherent, porous friable cake at loads of about 0.02–0.03 MN. The approximate dimensions of this cake are: diameter 55 mm, height 15 mm. Further compressive loading results in a relatively solid cake of compacted material which is friable at the edges and hard in the centre. The approximate dimensions of this final cake are: diameter 60 mm, height 10 mm. On dissecting the cake, the pebble is removed and found to have experienced a large, flattening strain.

The experimental method is essentially that of Bridgman's (1937) 'simple squeezer', for which the distribution of the stresses in the sample is not accurately known. Attempts to calculate the stresses (e.g. by Jamieson & Lawson 1962) suggest that the normal stresses are highest at the centre of the specimen, decreasing to atmospheric pressure at the jacket. This conforms with the general appearance of the final cake, but Gay & Jaeger (1975) found that pebbles placed some distance away from the centre of the specimen experienced equivalent strains to pebbles at the centre and, from the displacement of markers in the matrix, that the strain in the central region was homogeneous. These observations agree with Bridgman's (1937, p. 393) original suggestion that the pressure acting at any point in the sample approximates to the average applied pressure, i.e. the uniaxial compressive stress is reasonably uniformly distributed over the compacted cake. Use is made of this approximation later in the paper to calculate the axial stress acting on the samples at various applied loads, assuming a constant area for the cakes during loading. This assumption is supported by the very similar areas of the cakes at loads of 0.05 and 4.5 MN; an average cake diameter of 55 mm is used in the calculations.

(b) *Results*

The results of experiments on individual pebbles of different rock types in a matrix of marble showed that the amount of deformation experienced by the pebbles depended upon their relative strengths or ductility contrasts with the matrix. In particular, none of the pebbles changed shape during the initial deformation of the sample until the applied load exceed an apparent yield strength of the pebble and, after yielding, the amount of deformation experienced by the pebble relative to that experienced by the sample depended on the ductility contrast between the pebble and the matrix. Magnitudes of the apparent yield strengths are listed in table 1 and figure 2 compares the axial shortening experienced by the pebble with that experienced by the sample, after the initial coherent cake has been formed.

PHILOSOPHICAL TRANSACTIONS OF THE ROYAL SOCIETY A MATHEMATICAL, PHYSICAL & ENGINEERING SCIENCES

The graphs show that weak pebbles such as shale and sandstone deform slightly more than the composite samples do after yielding, possibly because of their very porous nature. By contrast, the more competent rocks such as marble and limestone deform slightly less and the strongest rocks, the oolitic limestone, trachyte and quartzite deform very much less than the matrix. Not evident on these graphs is the work hardening nature of the deformation process; the initial strains of both pebble and sample are achieved at relatively low loads but as deformation proceeds the load increment required for an equivalent strain increment becomes larger.

TABLE 1. YIELD STRENGTHS (Y) AND DUCTILITY CONTRASTS (R) OF THE DIFFERENT PEBBLES

pebble	matrix	Y (MN)	R
sandstone	marble	0.02	0.90
shale	marble	0.02–0.03	0.90
marble	marble	0.03	1.15
Solenhofen	marble	0.06	1.15
oolitic limestone	marble	0.04	1.45
trachyte	marble	0.07	1.50
quartzite	marble	0.09	2.00
Solenhofen	adamellite	0.03–0.04	?
Solenhofen	marble salt	0.10	?

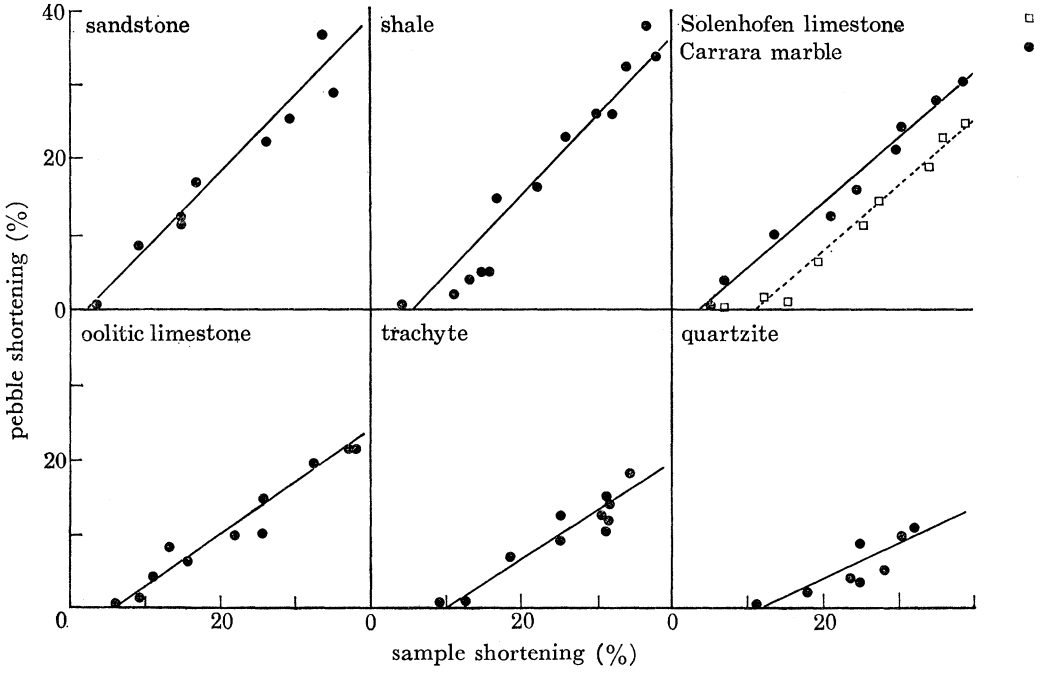

FIGURE 2. Graphs illustrating the deformation of pebbles of various rock types in a marble matrix during uniaxial compression of the composite samples (after Gay & Jaeger 1975).

A very important point which emerges from figure 2 is the approximately linear relation between the axial shortenings of the pebble and sample respectively, and the systematic decrease in the slope of this straight line with increasing strength. The slopes R of these lines provide a measure of the ratio of the ductility of the *matrix* to that of the *pebble*. The values of R computed in this way are also listed in table 1.

The influence of the composition of the matrix on a pebble of fixed rock type (Solenhofen limestone) is illustrated in figure 3. The pebble in the adamellite matrix yields almost immediately after the formation of the matrix cake (loads of 0.03–0.04 MN) but larger loads are required before yielding takes place in the more ductile marble and marble-salt matrices (see table 1). However, after yielding has occurred the pebbles deform at much the same rate in all three matrices, which denies any further influence of ductility contrast on pebble deformation. This surprising observation is thought by Gay & Jaeger (1975) to be due to the fact that all three matrices are essentially similar granular materials, rather than rocks with different strengths, at the low loads where much of the deformation occurs. The work-hardening nature of the deforming samples is clearly illustrated by the contours of equal load which are also plotted on figure 3.

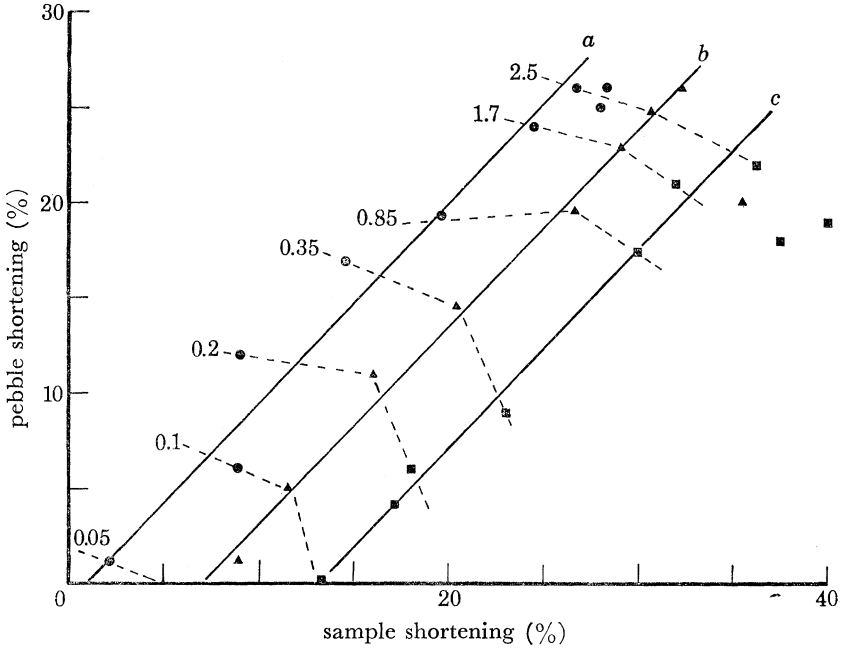

FIGURE 3. Graphs illustrating the deformation of pebbles of Solenhofen limestones in matrices of (*a*) adamellite; (*b*) marble; (*c*) marble-salt. The dashed lines are contours of load (in MN). (After Gay & Jaeger 1975.)

Figures 2 and 3 express the strains in the samples in terms of axial shortening because no estimates have been made of the elongations experienced by the composite sample. However, axial ratios, $\sqrt{(\lambda_1/\lambda_3)}$, and dilatations of individual deformed pebbles subjected to various loads are listed in table 2. The importance of the work-hardening nature of the deformation is again evident from the data, as is the large dilatation experienced by all the pebbles except those of shale. These large volume strains indicate that deformation probably takes place by cataclasis and evidence of this can clearly be seen in thin sections of the pebbles. The rocks made of strong brittle materials such as quartz and feldspar are cut by extension fractures, grain boundary fractures and shear planes. The carbonate rich rocks deform in a more ductile manner with the profuse development of up to two or three sets of twin lamellae but extension fractures, parallel to the axis of compression cut most grains and Lüders bands form in the very fine-grained Solenhofen limestone at high compressive loads.

FIGURE 4. An artificially deformed conglomerate: pebbles are (from left to right) Carrara marble; oolitic limestone and quartzite; Solenhofen limestone; shale; quartzite; and Solenhofen limestone. The pebbles are set in a matrix of mica schist and plaster of paris with an outer matrix of marble. (From Gay & Jaeger 1975.)

(*Facing p.* 115)

PHILOSOPHICAL TRANSACTIONS OF THE ROYAL SOCIETY A MATHEMATICAL, PHYSICAL & ENGINEERING SCIENCES

The response of the different pebbles to the deforming forces is illustrated in figure 4, plate 4, which shows a deformed artificial conglomerate. In this conglomerate, the shale pebble has deformed homogeneously (except where it is intruded by an adjacent quartzite pebble), as have the marble and limestone pebbles. The oolitic limestone is cut by several shear fractures and some oolites have been elongated and wrapped around a quartzite pebble, which, by contrast, is relatively undeformed except for being cut by extension fractures. The other quartzite pebble has been flattened by collapse along a shear plane. In this conglomerate, the different pebbles generally appear to have deformed in the same way as they do when deformed by themselves in a composite sample; the presence of the other pebbles and the resultant high concentration of pebbles to matrix does not appear to have influenced the strengths or ductility contrasts of the pebbles.

TABLE 2

load	sandstone		shale		marble		Solenhofen		oolitic limestone		trachyte		quartzite	
MN	R_a	D	R_a	D	R_a	D	R_a	D	R_a	D	R_a	D	R_a	D
0.02	1.01	1.0	1.00	0.0	.	.	.	.	.	.	.	.	.	.
0.03	1.18	8.5	1.05	2.0	1.03	4.5	.	.	.	.	.	.	.	.
0.04	1.24	8.5	0.09	4.0	.	.	.	.	1.01	3.5	.	.	.	.
0.05	1.28	8.0	1.32	5.0	1.11	7.5	1.00	0	1.04	7.5	1.00	0	.	.
0.06	.	.	.	.	.	.	1.04	4	.	.	1.01	2	.	.
0.075	.	.	.	.	1.24	11.0	1.03	2	1.10	10.0	1.02	2	1.00	0.0
0.09	.	.	.	.	.	.	.	.	.	.	.	.	1.01	3.5
0.10	1.41	13.0	1.33	3.5	1.31	14.0	1.16	15	1.18	13.0	1.07	9	1.03	7.5
0.20	1.60	18.0	1.52	7.5	1.39	17.0	1.25	12	1.24	13.0	1.20	14	1.10	14.0
0.35	1.68	15.0	1.58	4.5	1.53	12.5	1.36	15	1.40	23.0	1.28	20	1.16	17.0
0.83	1.69	5.0	1.73	2.0	1.60	12.0	1.47	21	1.52	23.5	1.32	22	1.25	30.0
1.65	2.02	2.0	1.84	0.3	1.75	14.0	1.60	15	1.60	23.0	1.38	23	1.29	21.0
2.50	.	.	2.01	0.3	1.83	14.5	1.63	13	1.65	20.0	1.45	16	1.41	35.0

$R_a = \sqrt{(\lambda_1/\lambda_2)}$, the axial ratio of the strain ellipsoid; calculated by averaging the observed maximum and intermediate quadratic elongations; the difference between these values was normally small.

D, dilatation (%).

DISCUSSION

(a) *Theoretical considerations*

This analysis of the experimental method assumes that both matrix and pebble behave as Bingham substances; i.e. they have finite yield strengths. Once these yield strengths are exceeded the matrix and pebble begin to deform independently at a rate of strain which depends on the plastic coefficients of viscosity.

Figure 5*a* illustrates the rheological elements of an ideal Bingham substance which does not work harden. The stress, σ_1, is applied to the Saint-Venant element, with yield strength Y, through the spring E_h and the motion of the element is resisted by the dashpot η_{pl}. If $\sigma < Y$ then the total strain is given by

$$\epsilon = \sigma/E_h.$$

If $\sigma > Y$, then at time t,

$$\epsilon = (\sigma - Y)\, t/\eta_{pl} + \sigma/E_h \quad \text{(Jaeger \& Cook 1969, p. 304)}.$$

For large finite strains the elastic component of strain can be ignored; i.e.

$$\epsilon = (\sigma - Y)t/\eta_{pl}. \qquad (1)$$

Consider the behaviour of the composite sample in figure 5*b*, under increasing uniaxial compressive load assuming that the sample and its components behave as Bingham substances. The pebble, A, has a yield stress Y_A and a coefficient of plastic viscosity η_A; similarly, for the matrix, B, the yield stress is Y_B and the plastic viscosity η_B. The strains experienced by each component are, respectively, ϵ_A and ϵ_B and it is assumed that the strain in the matrix is equivalent to the strain experienced by the composite sample itself. Continuity of stresses across the pebble–matrix interface and no slipping at the interface are assumed and the analysis only considers shortening strains parallel to the direction of maximum compression.

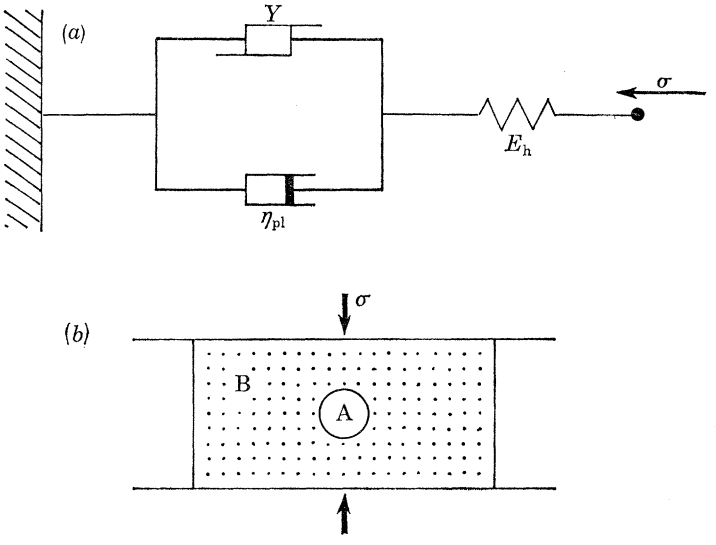

FIGURE 5. (*a*) Diagrammatic representation of the Bingham rheological body; σ-applied compressive stress. (*b*) Sketch of the ideal composite sample consisting of pebble A in matrix B; σ-applied compressive stress.

TABLE 3. DEFORMATION OF PEBBLE AND MATRIX COMPONENTS DURING INCREASING UNIAXIAL COMPRESSIVE STRESS

stress	time	strain in pebble	strain in matrix
Y_B	t_B	0	0
Y_A	t_A	0	$(t_A-t_B)\ (Y_A-Y_B)/\eta_B$
σ	t	$(t-t_A)\ (\sigma-Y_A)/\eta_A$	$(t-t_B)\ (\sigma-Y_B)/\eta_B$

Table 3 summarizes respective deformations of pebble and matrix with increasing stress and time. When the stress is less than the matrix yield stress, no deformation occurs. At time t_B, the applied stress equals the yield stress, Y_B, of the matrix which begins to deform. As the stress increases to Y_A the matrix experiences a finite strain which can be calculated from equation (1). Similarly, at time t_A, when $\sigma = Y_A$, the pebble begins to deform and when the applied stress reaches its maximum value σ at time t the strains experienced by the pebble and matrix, respectively, are:

$$\epsilon_A = (t-t_A)\ (\sigma-Y_A)/\eta_A, \tag{2a}$$

$$\epsilon_B = (t-t_A)\ (\sigma-Y_A)/\eta_B + (t_A-t_B)\ (Y_A-Y_B)/\eta_B$$

$$= (t-t_B)\ (\sigma-Y_B)/\eta_B. \tag{2b}$$

The equations are depicted graphically in figure 6*a*.

Equations 2 can be rearranged to give the following equation relating the strain experienced by the pebble to that experienced by the matrix or composite sample:

$$\epsilon_A = \frac{\eta_B}{\eta_A}\epsilon_B - \frac{(t_A - t_B)(Y_A - Y_B)}{\eta_A}. \quad (3)$$

This equation is plotted in figure 6*b*.

The strain in the pebble compared to that in the composite sample depends solely on the ratio of the plastic viscosities (η_A/η_B); the larger this ratio, the smaller is the change in pebble shape. This influence of viscosity ratio is very similar to that described by Gay (1968) for particle-matrix systems of Newtonian fluids. However, the Bingham substances discussed here have finite yield strengths and equation (3) shows that no pebble deformation occurs until the matrix has been deformed by a finite amount which depends on the yield strength of the matrix and pebble and on the plastic viscosity of the matrix. The straight line graph in figure 6*b* is similar to those graphs in figure 2 for the deformation of spheres and cylinders of rock in a granular matrix.

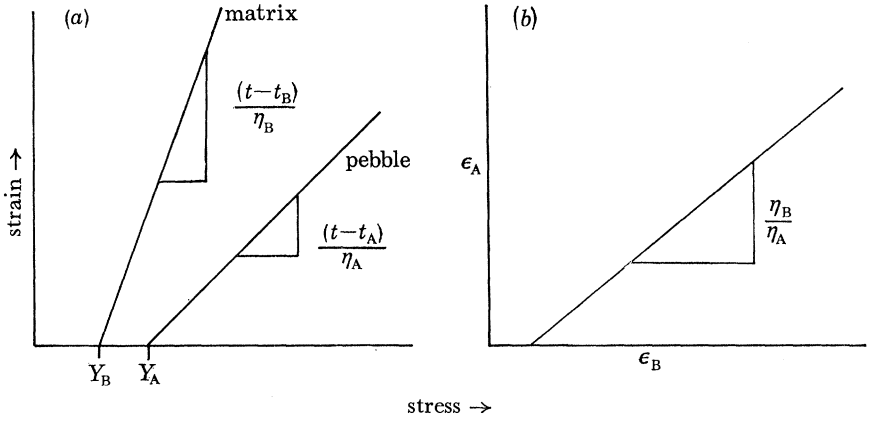

FIGURE 6. (*a*) Graphs showing the stress–strain behaviour of matrix and pebble as calculated from equations (2). (*b*) Graph showing the variation in strain experienced by the pebble (ϵ_A) and matrix (ϵ_B) as calculated from equation (3).

Gay & Jaeger's (1975) experiments showed that the lithic samples used by them behaved in a more complex way than the ideal Bingham substances assumed in the above analysis. In particular, the samples strain or work hardened and required increasingly larger load increments to obtain equal increments of strain. The rate of work hardening was approximately the same in both the matrix and the pebble, so that the graphs relating the total finite strain in the sample to that in the pebble are approximately linear.

This behaviour approximates to that of the generalized Bingham substance (Reiner 1969, p. 278) in which the coefficient of plastic viscosity increases with increasing strain, a response similar to that exhibited by flour dough (Schofield & Scott Blair 1933) and pitch (Trouton 1906).

Some idea of the magnitudes of these changes in coefficient of viscosity can be obtained from the Levy–Mises equation of plastic flow:

$$\delta\bar{\epsilon}_1 - \delta\bar{\epsilon}_3 = \psi(\sigma_1 - \sigma_3) \quad \text{(Ford 1963, p. 410)},$$

where $\delta\bar{\epsilon}_1$, $\delta\bar{\epsilon}_3$ are the increments in natural strain, σ_1 and σ_3 are the maximum and minimum principal stresses, and ψ is the plastic proportionality constant. In the present analysis, σ_3 is unknown and because we are concerned with changes in ψ during increments in applied load, it is logical to modify the equation to

$$\delta\bar{\epsilon}_1 - \delta\bar{\epsilon}_3 = \psi\delta\sigma \tag{4}$$

where $\delta\sigma$ is the stress increment causing the strain increments.

For the experimental data, $\delta\bar{\epsilon}_1$, $\delta\bar{\epsilon}_3$ are calculated from the axial ratios $\sqrt{(\lambda_1/\lambda_3)}$ of the deformed pebbles and $\delta\sigma$ from the load increments (assuming constant sample area) listed in table 2. The variation in ψ with load and total strain is plotted for three rock types in figure 7*a*, *b*. These graphs quite clearly show a marked decrease in ψ from values larger than 10 to smaller than 0.10 with increasing load and finite strain. There is no direct relation between ψ and the coefficient of plastic viscosity but by comparing the dimensions of ψ and η_{pl} it can be shown that for a fixed time ψ is proportional to $(1/\eta_{\mathrm{pl}})$. Thus, the observed changes in ψ indicate a hundredfold increase in the coefficient of viscosity of the composite samples during deformation.

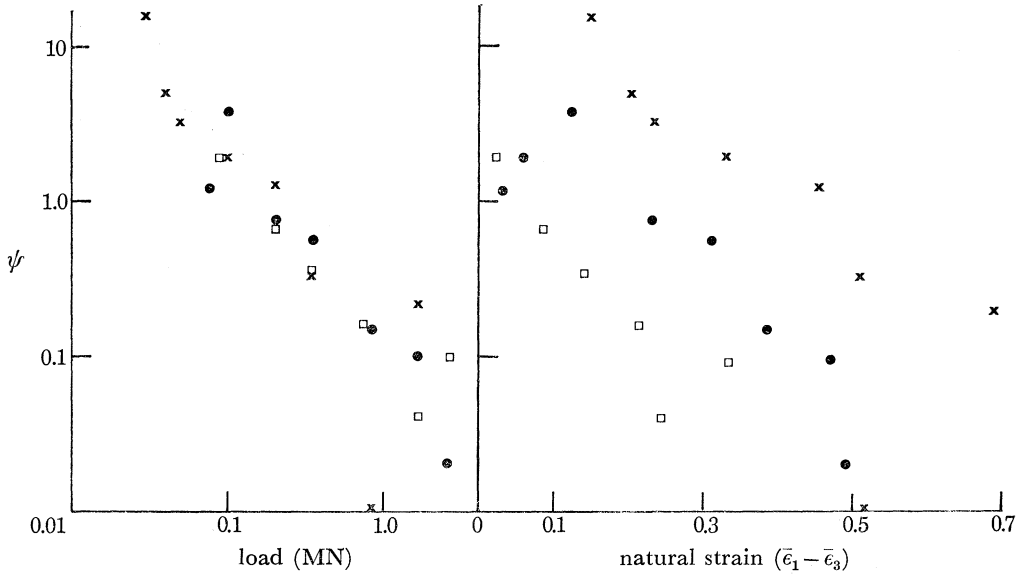

FIGURE 7. Graphs showing the variation of plastic proportionality constant (ψ) with (*a*) applied load; and (*b*) natural strain. □, quartzite; •, Solenhofen; ×, sandstone.

(*b*) *Geological implications of the experimental results*

(i) *Yield strength of the pebbles*

The experiments showed that there was a minimum value of the applied load below which the pebble did not deform. This observation that a pebble has a finite yield strength, which must be exceeded for deformation of the pebble to occur, is likely to be important in nature, and probably explains the presence of apparently undeformed pebbles in moderately deformed conglomerates.

However, more important are the small magnitudes of the loads at which yielding begins. The resultant apparent yield stresses calculated from these loads, assuming an average area (2375 mm², for a diameter of 55 mm) for all samples, range from 10 to 42 MPa. Because of the

porosity in the matrix, the pebble carries more of this load than the surrounding material and thus the calculated stresses underestimate the true stress at which the pebble is yielding. However, the calculation of the average stress acting on the sample remains valid.

The apparent yield stresses are equivalent to overburden stresses at depths of less than 2 km in the Earth's crust. Even allowing for differences between the experimental conditions and those in nature, it seems likely that pebbles will begin to deform under conditions of diagenesis at relatively shallow depths. This supports Dunnet & Siddans' (1971) conclusion that pretectonic deformation may occur by gravitational compaction.

(ii) *Ductility contrast*

The ductility contrast controls the rate at which the pebbles deform relative to the deformation experienced by the sample as a whole. For example, figure 2 shows that at 30 % sample shortening, a shale or sandstone pebble would have experienced a 25 % axial shortening compared with 10 % for a quartzite pebble. Moreover, the values of R, the ductility contrast between matrix and pebble, listed in table 1 are very similar to the viscosity contrasts between pebble and matrix deduced by Gay (1969) from deformed pebbles in natural conglomerates assuming a viscous model. This suggests that at higher temperatures and pressures the viscosity contrast will be the controlling factor in the deformation of pebbles.

However, the viscous theory developed by Gay (1968) predicted that with increasing pebble concentration the average coefficient of viscosity for the whole rock would increase and the viscosity contrast between individual pebbles and the rock would tend to unity. Analysis of the deformed pebbles in the artificial conglomerate illustrated in figure 4, suggests that this

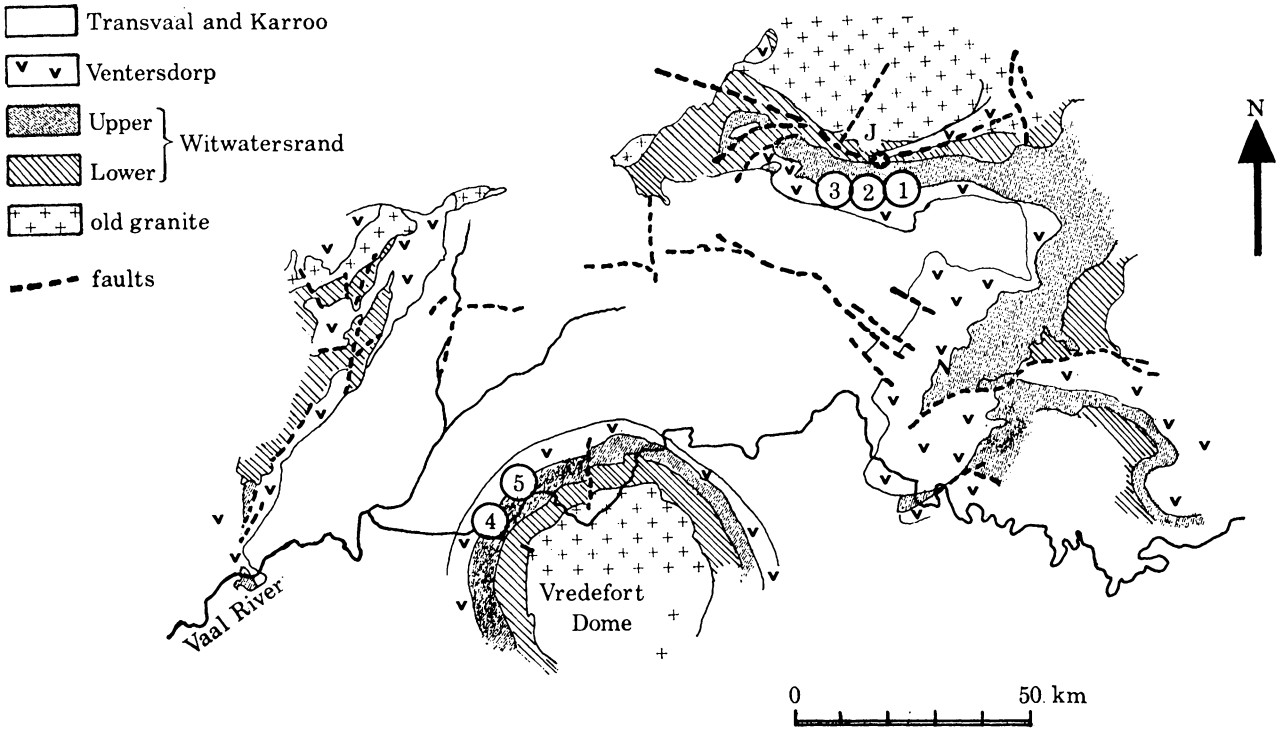

FIGURE 8. Simplified geological map of the area south of Johannesburg (J); 1–5 are localities at which pebble measurements were made. (After Du Toit 1954.)

reduction is not important in the present experimental conditions. In the conglomerate (which was subjected to a load of 4.50 MN, equivalent to a stress of about 750 MPa) the pebbles are 5–10 % more eccentric than single pebbles deformed to approximately the same load. This increase in eccentricity is probably not statistically significant, especially when it is noted that some of the pebbles (e.g. quartzite) are much less deformed than expected and that the overall deformation in the conglomerate is inhomogeneous.

(iii) *Work hardening*

The work hardening nature of the deformation is important in that it imposes a limit on the amount of deformation which can take place during diagenesis. Examination of the axial ratios listed in table 2 shows that a considerable change in pebble shape occurs under a load of 0.35 MN. This is equivalent to an average stress of 140 MPa on the specimen, which corresponds to a depth of about 5–6 km. The next load increment 0.83 MN is equivalent to a stress of 350 MPa or a depth of 14 km; this pressure is probably too large to be achieved during diagenesis. The axial ratios of the deformed pebbles at these loads range from about 1.2 to 1.6 depending upon pebble composition and these seem to be reasonable values of the maximum deformation likely to be achieved by gravitational compaction. These numbers agree well with the pre-tectonic strain of 1.3:1 reported by Dunnet & Siddans (1971) for a deformed pisolite tuff.

(c) *Geological example: deformed pebbles in the Elsburg Reefs of the Upper Witwatersrand System, South Africa*

The localities at which pebbles were collected for strain measurements are shown in figure 9, which is a simplified geological map of the area south of Johannesburg; all the sampling sites were in approximately the same stratigraphic position.

The northernmost localities (1, 2, 3) were sited on the shallow dipping, right way up edge of the basin and the southern sites on the overturned horizons around the Vredefort dome. The sites on the northern rim of the basin were chosen because the host rocks are apparently undeformed and are unlikely to have had more than 7–8 km of cover rocks overlying them. In other words the P, T conditions are unlikely to have been sufficiently extreme for the rocks to have become viscous since deposition of the conglomerate. However, at least some of the pebbles in the conglomerate have undoubtedly been through more than one cycle of sedimentation and may have been previously tectonically deformed, or been derived from tectonically deformed rocks, lower in the Witwatersrand sequence. In particular, the pebbles from sites 2 and 3 have a provenance to the northwest of Johannesburg where the Witwatersrand sediments are quite severely folded and faulted (Mellor 1913; Roering 1968).

The pebbles at all three localities are generally well rounded and comprise between 25 and 35 % of the individual conglomeratic horizons. The majority of them are quartz or quartzite in composition but a few chert pebbles also occur. They range in size from 20 to 120 mm in diameter and are set in a coarse-grained quartzitic matrix with rounded to sub-angular grains of quartz, much finer-grained secondary quartz and sericite or muscovite (figure 11*a*). The rock carries no tectonic or metamorphic fabric and, on the presence of sericite, appears to have been metamorphosed to lower greenschist facies during diagenesis. Up to 20 % of the quartz grains show undulose extinction and may contain one or more sets of deformation lamellae; presumably these structures reflect grain deformation during an earlier period of Witwatersrand time.

PHILOSOPHICAL TRANSACTIONS OF THE ROYAL SOCIETY A MATHEMATICAL, PHYSICAL & ENGINEERING SCIENCES

The two sites (4, 5) on the southern rim of the basin differ markedly from those described above. The strata at these sites are overturned and dip southeast at 50–60°. A cleavage is developed at locality 5 and at both localities the matrix is seen to consist mainly of quartz grains, which are cut by sets of deformation lamellae and planar features. In addition, the pebbles are much more deformed than at localities 1, 2 and 3, although there is no development of a preferred orientation of long axes (cf. figure 9). The composition of the pebbles is normally quartz or quartzite.

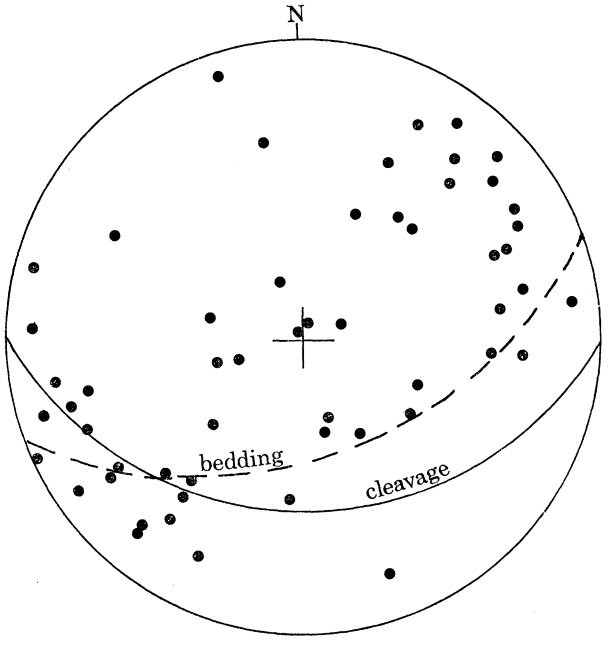

FIGURE 9. Equal-area, lower hemisphere stereographic projection of pebble long axes in relation to the bedding and cleavage planes; locality 5; 57 points.

The axial ratios of at least 28 pebbles were measured at each site and at sites 3, 4 and 5 the orientations of the pebble axes were also recorded. These data were used to compute the axial ratios of the strain ellipsoid and the initial pebble, by Ramsay's (1967, pp. 211–216) analytical technique. The results of these calculations are listed in table 4 with values of Lode's parameter ν, which is used to describe the symmetry of the strain ellipsoids, and is calculated from the axial ratios by using the equation

$$\nu = [\lg(\lambda_2/\lambda_3) - \lg(\lambda_1/\lambda_2)]/\lg(\lambda_1/\lambda_3).$$

The results for each set of pebbles are plotted in figure 10 on a logarithmic deformation plot (Flinn 1965; Gay 1969, p. 392).

The results are most complete for locality 1 where data for chert, quartz and quartzite pebbles are available. All three types of pebbles have experienced essentially the same flattening finite strain. The flattening nature of this strain suggests that some of it at least may be due to compaction during gravitational loading. This is born out by the oblate shape of the pebbles themselves and by some of the internal structures seen in thin section. Of the pebbles examined under the microscope, some are made up of good recrystallized quartz polygons; others are comprised of interlocking grains with sutured, boundaries and a preferred orientation of long

axes; and in others the original grains are still visible. Deformation lamellae, bands and undulose extinction in the quartz grains are also common; these structures presumably represent earlier episodes of tectonic deformation. However, of importance here is the presence of small healed cracks, marked by trains of dust and fluid inclusions, which cut grains or follow grain boundaries and are aligned close to the direction of maximum shortening. These cracks resemble extension cracks which cut the experimentally deformed pebbles.

TABLE 4. TECTONIC STRAINS EXPERIENCED BY DEFORMED PEBBLES IN THE ELSBURG REEFS

locality	pebble type	N	$\sqrt{(\lambda_1/\lambda_2)}$	$\sqrt{(\lambda_2/\lambda_3)}$	$\sqrt{(\lambda_1/\lambda_3)}$	ν
1	chert	28	1.35	1.62	2.18	+0.23
	quartzite	264	1.37	1.67	2.28	+0.24
	quartz	260	1.42	1.73	2.45	+0.22
2	quartzite	245	1.42	1.58	2.25	+0.13
	quartz	402	1.56	1.46	2.26	−0.08
3	mixed	50	1.59	1.56	2.48	−0.02
4	quartzite	47	2.80	2.69	7.53	−0.02
5	quartzite	58	2.46	2.56	6.30	+0.02

N, number of pebbles measured.

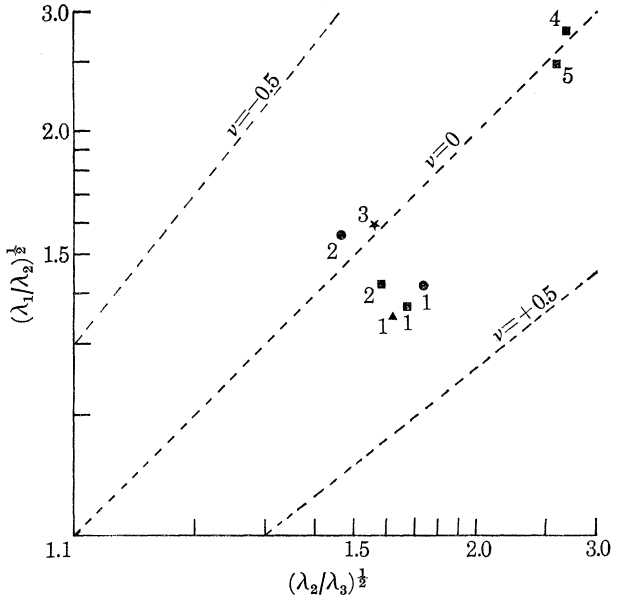

FIGURE 10. Deformation plot of the strain ellipsoids calculated from the deformed pebbles at localities 1–5. ●, quartz; ■, quartzite; ▲, chert; ★, mixed.

DESCRIPTION OF PLATE 5

FIGURE 11. Photomicrographs of samples from the Elsburg reefs; (scale bars = 1 mm; all pebbles have short axes perpendicular to the scale bar). (*a*) Matrix from conglomerate at locality 2; thin section not oriented; plane polarized light. (*b*) Healed and open cracks in a quartzite pebble from locality 2; the wide crack on the left hand side is filled with opaque material (plane polarized light). (*c*) Healed cracks cutting recrystallized quartz grains in a quartzite pebble from locality 3 (crossed polarizers). (*d*) Closely spaced conjugate shear planes in a quartzite pebble from locality 5. New quartz is growing along some of the shear planes (crossed polarizers). (*e*) Closely spaced shear planes with associated feather fractures cutting healed cracks in a quartzite pebble from locality 4 (plane polarized light). (*f*) New quartz developed along part of a healed crack in a quartzite pebble from locality 5 (crossed polarizers).

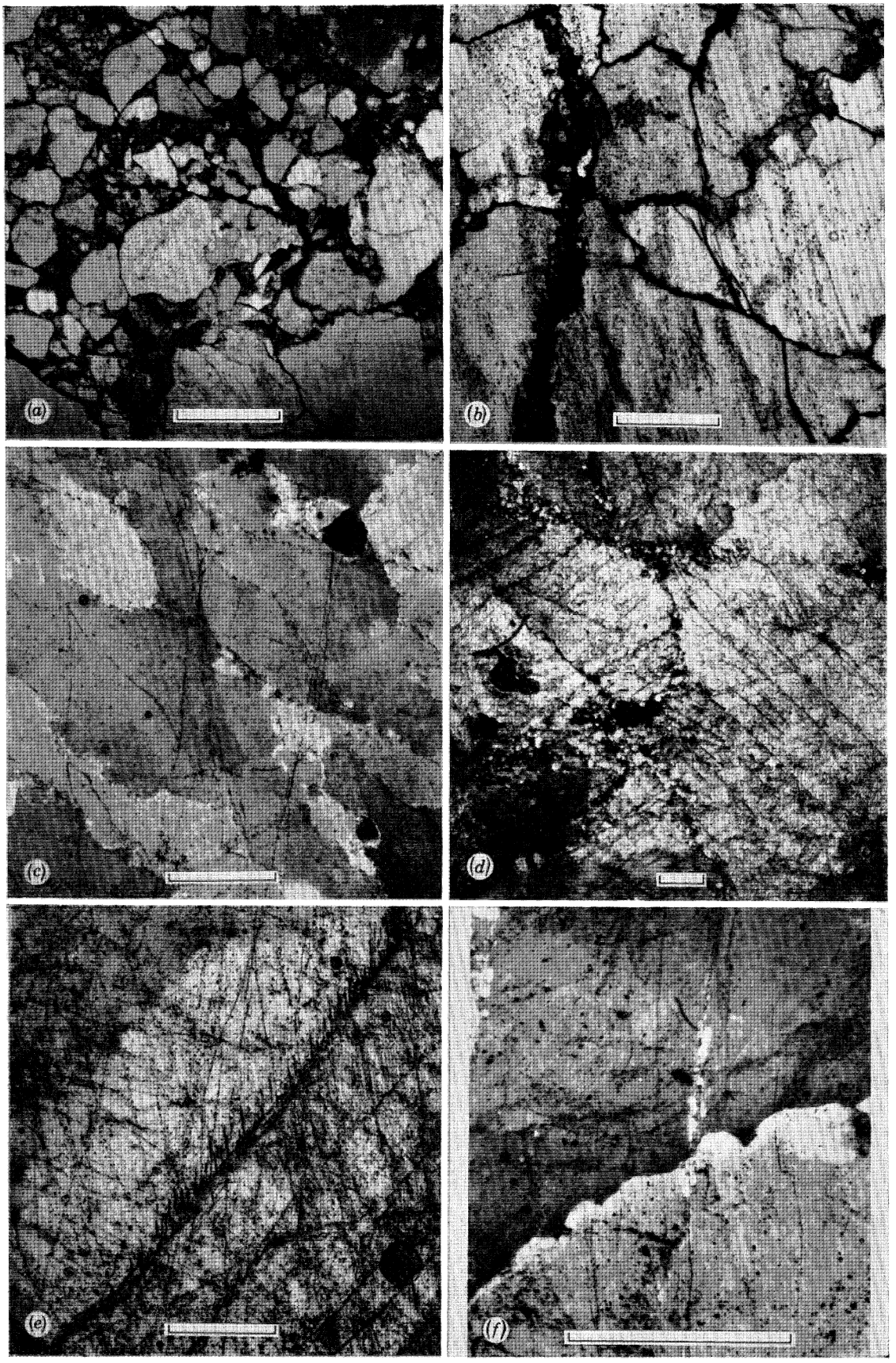

FIGURE 11. For description see opposite.

(*Facing p.* 122)

PHILOSOPHICAL TRANSACTIONS OF THE ROYAL SOCIETY A MATHEMATICAL, PHYSICAL & ENGINEERING SCIENCES

At locality 2, the quartzite pebbles indicate a flattening type strain but those of quartz lie close to the line for a pure shear plane strain. As at locality 1, most of the pebbles seen in thin section, contain evidence of previous deformation, such as lamellae and undulose extinction. In addition, the quartz pebbles have a very strong fabric of recrystallized, elongated quartz grains sub-parallel to the major pebble axis. This suggests that the observed pure shear strain ellipsoid reflects not only the deformation associated with the diagenesis of the Elsburg reefs but also a previous deformation history. However, healed cracks (figure 11*b*) marked by bubble trains and filled with iron oxides are visible in most thin sections (especially quartzite); these cracks often cut across recrystallized grains and indicate a possible cataclastic deformation during lithostatic loading.

Similarly, the strain at locality 3 is of a pure shear type and again the pebbles are made up of recrystallized grains of quartz which define a planar fabric and contain deformation lamellae and bands. The provenance of the pebbles is the same as that for locality 2 and the observed symmetry of the strain ellipsoid may reflect a previous strain history. However, as at localities 1 and 2, healed cracks (figure 11*c*) cut across individual grains at high angles to the maximum and intermediate pebble axes. Some of these cracks now contain new quartz.

The finite strains experienced by the pebbles at localities 4 and 5 are of a similar pure shear type to those at localities 2 and 3 but the magnitudes are very much greater. These sites are situated on the overturned limb of the synclinorium around the Vredefort Dome. The overturning post-dates the lithification of the sediments and hence any pebble deformation accompanying the diagenesis will have superimposed on it deformational features accompanying the overturning.

On a microscopic and hand-specimen scale, these younger deformational features are intense. Many of the pebbles at both localities are cut by conjugate pairs of closely spaced shear planes, very similar to Lüders bands. In addition, at site 5, contiguous pebbles are often found to be pitted by pressure solution at their points of contact. The shear planes are symmetrically distributed about the long axes of the pebbles with the angles between them varying from about 60 to 130° in individual pebbles. In thin section, new relatively strain-free quartz is often found along the shear planes (figure 11*d*) and feather fractures cut the grains immediately adjacent to some shear planes (figure 11*e*). Deformation lamellae and other planar features are ubiquitous and normally two or more sets are present. Healed cracks, marked by dust or bubble trains, are found in some pebbles sub-parallel to the long axes.

None of these features are likely to be compatible with deformational structures due to gravitational loading but in some sections, healed cracks at angles of 0–30° to the axis of maximum shortening are seen. These cracks are marked by irregular trains of inclusions and are normally discontinuous and slightly wavy in appearance. Displacement of the cracks across shear planes can occasionally be seen and new quartz may be developed along them (figure 11*f*) especially in pebbles which have shear planes inclined at large angles (120°) to their long axes.

The correlation of these irregular cracks with extension fractures likely to be induced in the pebbles during gravitational loading seems correct in view of the fact that the later deformation does not appear to have changed the relative positions of the pebbles; i.e. the pebbles still tend to lie with their long axes in the bedding plane, as they would have been deposited during formation of the conglomerates. The presence of the closely spaced shear planes or Lüders bands

PHILOSOPHICAL TRANSACTIONS OF THE ROYAL SOCIETY A MATHEMATICAL, PHYSICAL & ENGINEERING SCIENCES

and the growth of new quartz indicates that the superimposed deformation took place under conditions of fairly high confining pressures and temperatures which would preclude the development of cataclastic features such as extension cracks.

Conclusions

The experimental work outlined in the first part of this paper suggested that it might be possible to achieve fairly large finite strains in pebbles during gravitational compaction of sediments at low pressures and temperatures. In these experiments, the samples of matrix and pebbles behave as work hardening Bingham bodies; deformation only proceeds after the yield strength of the pebble has been exceeded and the subsequent finite strain depends on the ductility contrast between the pebbles and the host rock. Applying these results to natural conglomerates, one would expect to find deformed pebbles in all conglomerates which have been subjected to overburden pressures of 100–200 MPa, equivalent to a sedimentary cover of 4–8 km. Ideally, spherical pebbles should deform to oblate spheroids but because pebbles are normally ellipsoidal in shape, it is more likely that after deformation they would be flattened in the bedding plane and have three unequal principal axes. Because of the work hardening nature of the deformation during compaction, the deformations are unlikely to be extreme; the experimental results suggest maximum pebble axial ratios of 1.2–1.6 for initially spherical pebbles of varying composition. Microscopic structures which might be used to identify this type of deformation in deformed conglomerates include extension cracks and grain boundary cracks parallel to the short axes of pebbles of quartzite or other brittle rocks and twin lamellae in pebbles of carbonate rocks.

The Elsburg reefs which crop out south of Johannesburg at the top of the Upper Witwatersrand System, appear to be suitable conglomeratic horizons in which to look for evidence of deformation of pebbles by gravitational compaction. These conglomerates contain pebbles of quartz, quartzite and chert which have been derived from the underlying sediments and conglomerates. Accordingly the pebbles may well have been deformed during earlier tectonic events but after deposition in the Elsburg reefs they have probably only been subjected to maximum temperature of 200 °C and overburden pressures of 200 MPa, compatible with a sedimentary cover of 7–8 km. The finite strain ellipsoid deduced from the pebbles at locality 1 plots in the flattening region of the deformation plot as expected and in thin section healed cracks can be seen sub-parallel to the short axis of the pebbles. However, the maximum strain ratio, $\sqrt{(\lambda_1/\lambda_3)}$, is larger than expected from the experiments; this may be due in part to previous deformations. The pure shear type of strain and the larger axial ratios deduced from the pebbles at localities 2 and 3 are also thought to reflect the influence of deformations in pre-Elsburg times but, again, healed cracks which are compatible with deformation during diagenesis can be identified.

On the southern side of the Witwatersrand basin, at localities 4 and 5, the Elsburg reefs have been deformed during post-lithification overturning of the sediments. This superimposed deformation has resulted in the development of Lüders bands, deformation lamellae and planar features in the pebbles and the growth of new quartz. However, still visible in thin sections of the pebbles are irregular, wavy, healed cracks which are sub-parallel to the short pebble axis and which are thought to represent extension cracks induced into the pebbles during the lithification of the conglomerates.

These observations support the validity of the experimental results. It seems likely that significant pre-tectonic deformations can occur during lithification of the sediments. The magnitudes of these deformations will depend on the relative yield strengths of, and ductility contrasts between the deforming particles and the host rock.

Tectonic strains superimposed on these lithostatically deformed pebbles are likely to take place at conditions of higher temperature ($> 300\ ^\circ C$) and pressure (> 200 MPa). In this environment most rock types will tend to behave like viscous fluids and deform by secondary (steady state) creep (Heard 1976; Flinn 1965). The important factors controlling the relative deformation of the individual pebbles and the host rock would be the long term yield strengths (Price 1964) of the pebbles and the viscosity contrasts between the pebbles and rock once steady state creep had been initiated.

J. C. Jaeger devised the experimental method used to obtain the results discussed in this paper and made the deformed conglomerate illustrated in figure 4. L. O. Nicolaysen read the manuscript and suggested some improvements.

References (Gay & Fripp)

Anhaeusser, C. R. 1974 *Infor. Circ. No.* 94, Econ. Geol. Res. Unit, Univ. Witwatersrand, Johannesburg.
Bridgman, P. W. 1937 *Proc. Am. Acad. Arts Sci.* **71**, 387–459.
Du Toit, A. L. 1954 *The geology of South Africa* (*3rd edition*). Edinburgh: Oliver & Boyd.
Dunnet, D. & Siddans, A. W. B. 1971 *Tectonophysics* **12**, 307–325.
Flinn, D. 1956 *J. Geol.* **64**, 480–505.
Flinn, D. 1965 In *Controls of metamorphism* (ed. S. W. Pitcher & G. W. Flinn), pp. 46–72. Edinburgh: Oliver & Boyd.
Ford, H. 1963 *Advanced mechanics of materials*, London: Longmans.
Gay, N. C. 1968 *Tectonophysics* **5**, 211–234, 295–302.
Gay, N. C. 1969 *J. Geol.* **77**, 377–396.
Gay, N. C. & Jaeger, J. C. 1975 *Tectonophysics* **27**, 303–322.
Handin, J. 1966 *Mem. Geol. Soc. Am.* **97**, 289.
Hasan, Z.-U. & Sarkar, S. N. 1967 *Norsk Geol. Tidssk.* **47**, 159–170.
Heard, H. C. 1976 *Phil. Trans. R. Soc. Lond.* A **283**, 173–186 (this volume).
Hossack, J. R. 1968 *Tectonophysics* **5**, 315–339.
Jaeger, J. C. & Cook, N. G. W. 1969 *Fundamentals of rock mechanics*. London: Methuen.
Jamieson, J. C. & Lawson, A. W. 1962 *J. appl. Phys.* **33**, 776–780.
Mellor, E. T. 1913 *Trans. Geol. Soc. S. Africa* **16**, 1–32.
Mukhopadhyay, D. & Bhattacharya, S. 1969 *J. geol. Soc. India* **10**, 77–87.
Oftedahl, C. 1948 *J. Geol.* **56**, 476–487.
Price, N. J. 1964 *Int. J. Rock. Mech. Mining Sci.* **1**, 277–303.
Ramsay, J. G. 1967 *Folding and fracturing of rocks*. New York: McGraw-Hill.
Reiner, M. 1969 *Deformation, strain and flow* (*3rd edition*). London: H. K. Lewis.
Robertson, E. C. 1972 In *The nature of the solid earth* (ed. E. C. Robertson *et al.*), pp. 631–659. New York: McGraw-Hill.
Roering, C. 1968 *Inform. Circ. No.* 48. Econ. Geol. Res. Unit, Univ. Witwatersrand, Johannesburg.
Schofield, R. K. & Scott Blair, G. W. 1933 *Proc. Roy. Soc. Lond.* A **139**, 557–566.
Trouton, F. T. 1906 *Proc. R. Soc. Lond.* A **77**, 426–440.
Winkler, H. G. F. 1967 *Petrogenesis of metamorphic rocks* (*2nd edition*). Berlin: Springer-Verlag.

Discussion

B. A. Bilby and M. L. Kolbuszewski (*Theory of Materials, University of Sheffield, Mappin Street, Sheffield, S1 3JD*). We should like to draw the attention of Dr Gay and other geologists to some theoretical work carried out in this department on the slow deformation of inhomogeneous

regions in incompressible viscous materials. We were first led to consider this problem in connexion with the homogenization of glass melts, and some results obtained by Eshelby on the deformation of an elliptic cylinder have already been reported briefly (Cable 1968). Our general method is to use the analogy between slow viscous incompressible flow and linear elasticity, together with the theory of the deformation of the elastic ellipsoidal inhomogeneity (Eshelby 1957, 1960) to discuss the finite deformation of an ellipsoidal inhomogeneity having a viscosity μ_1 differing from the viscosity μ of the matrix. In a forthcoming paper (Bilby, Eshelby & Kundu 1975) the deformations of elliptic cylinders and prolate and oblate spheroids under pure shear are treated. The progress of the deformation of the cylinder is conveniently described by the parameter $S = \ln (a/a_0)$, where a is the major axis of the elliptical cross section at any stage, and a_0 the value of a when the cross section is a circle. If S_H is the value of S when $\mu_1 = \mu$, the relation between S and S_H indicates the influence of the viscosity ratio $R = \mu_1/\mu$ on the deformation which occurs in the inhomogeneity. It is found (Cable 1968) that the relation between S and S_H is

$$S + \tfrac{1}{2}(R-1) \tanh S = S_H \qquad (1)$$

which is not linear, but reduces for S sufficiently small to the linear relation $(R+1)S = 2S_H$. In contrast, Gay (1968) finds the linear relation $(3+2R)S = 5S_H$. In fact, the method used by Gay is appropriate only for the initial deformation of a circular inhomogeneity. If applied correctly his method would give the linear relation with slope $2/(R+1)$, appropriate for small S in our theory, but because of technical errors Gay obtains a linear relation with the wrong slope. We believe, therefore, that some caution is necessary in deducing matrix strains from measurements on inhomogeneities of different viscosity, particularly when the strains are large. It is interesting to note that for large S the nonlinear relation (1) becomes $S_H = S + \frac{1}{2}(R-1)$. Such a relation resembles qualitatively the curves shown by Dr Gay at this meeting, although it strictly applies to a much simpler geometry than obtained in his experiments. The application of the general theory to more complicated geometries has been further discussed by Brierley & Howard and by ourselves, and the results will be published shortly.

References

Bilby, B. A., Eshelby, J. D. & Kundu, A. K. 1975 *Tectonophysics* **28**, 265–274.
Cable, M. 1968 Proceedings of the VIIIth International Congress on glass, p. 163.
Eshelby, J. D. 1957 *Proc. R. Soc. Lond.* A **241**, 376.
Eshelby, J. D. 1960 *Prog. Solid Mech.* **2**, 89.
Gay, N. C. 1968 *Tectonophysics* **5**, 211, 295.

N. C. Gay. I would like to thank Professor Bilby and Dr Kolbuszewski for contributing to the discussion of Mr Fripp's and my paper. I was particularly interested to learn of the theoretical results obtained by them and co-workers on the deformation of inhomogeneous regions in incompressible viscous materials, a problem which I attempted to solve (Gay 1968) in order to determine total finite strains in deformed conglomerates.

Bilby & Kolbuszewski point out that the linear relation derived by me to relate the strain in the inhomogeneity with that in the surrounding matrix is incorrect and is really only applicable for small strains. I have not been able to verify this statement of theirs nor have I found any technical errors in my argument to which they allude. My attempts to do this have been hampered by the fact that I have not been able to obtain copies of the papers by Cable (1968) and Bilby *et al.* (1975) in which the results quoted by Bilby & Kolbuszewski are derived.

In view of this apparent impasse, and because I was able to verify my equation experimentally and have since used it to obtain reasonable values of finite strain in deformed conglomerates (Gay 1969), I now intend to compare the different results empirically.

In figure 12, I have plotted graphs of the functions (Bilby & Kolbuszewski's notation):

$$S+\tfrac{1}{2}(R-1)\tanh S = S_{\mathrm{H}} \quad \text{(Cable 1968)} \tag{1}$$

$$(R+1)S = 2S_{\mathrm{H}} \quad \text{(Bilby \& Kolbuszewski)} \tag{2}$$

$$(3+2R)S = 5S_{\mathrm{H}} \quad \text{(Gay 1968)} \tag{3}$$

for $R = 2.5$. In these graphs, the strains in the inhomogeneity and matrix are plotted as the ratio (a/a_0), $(a/a_0)_{R=1}$ and (a/b) where (a/a_0) is the strain parameter used by Bilby & Kolbuszewski and (a/b), the ratio between the major and minor principal axes of the elliptical inhomogeneity, is the parameter used by me. These ratios are calculated from the natural strains $S = \ln (a/a_0)$, etc. I selected $R = 2.5$ because most pebbles in deformed rocks are probably less than 2.5 times more viscous than their host rock during deformation. Also plotted on this graph are the experimental points determined by me (Gay 1966, table Xb, p. 204) using ethyl cellulose – benzyl alcohol solutions to represent the inhomogeneity and matrix.

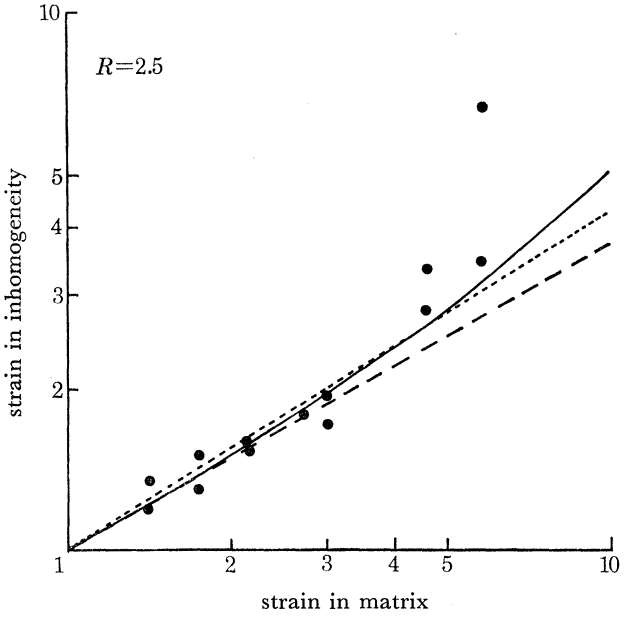

FIGURE 12. Variation between the strain in an inhomogeneity and the surrounding matrix as calculated from: equation (1), solid line; equation (2), large dashed line; equation (3), small dashed line. R is the viscosity ratio between the inhomogeneous particle and the matrix. Dots are experimental points determined by Gay (1966).

Quite clearly all three curves are similar at strain ratios < 3 and the curves for equations (1) and (3) agree well for a matrix strain $\leqslant 5$. The scatter on the experimental results is sufficiently large for the results to fit all three curves but they probably correlate best with equation (1), the exact solution determined by Cable (1968).

The effect of changing the value of R is illustrated in table 5, in which are listed values of the natural strains in the matrix, S_{H}, calculated from equations (1) and (3) for two different values of S, the natural strain in the inhomogeneity. At the lower strain level ($S = 1$) the differences

between the results from the two equations are insignificant for $R \leqslant 5$ although equation (3) always overestimates the magnitude of the matrix strain. Similarly at the higher strain level ($S = 2$) equation (3) gives larger values of S_H than does equation (1), but here the differences are certainly significant.

These observations indicate that although my equation may be incorrect, the strain values calculated by using it do not differ significantly from those predicted by Cable's (1968) equation for matrix strain ratios as large as 5 ($S \approx 1.6$) and viscosity ratios less than 5. These conditions cover most reported strains in deformed rocks known to me.

TABLE 5. MATRIX STRAINS, S_H, CALCULATED FROM EQUATIONS (1) AND (3) FOR VARIOUS VALUES OF R, ASSUMING (*a*) $S = 1$; (*b*) $S = 2$

	(*a*)		(*b*)	
R	equation (1)	equation (3)	equation (1)	equation (3)
1	1	1	2	2
2	1.38	1.40	2.48	2.80
3	1.76	1.80	2.96	3.60
4	2.14	2.20	3.45	4.40
5	2.52	2.60	3.93	5.20
7.5	3.48	3.60	5.13	7.20
10	4.43	4.75	6.82	9.20

Bilby & Kolbuszewski also suggest that the form of equation (1) for large S, namely

$$S_H = S + \tfrac{1}{2}(R-1) \tag{4}$$

resembles the curves published by Mr Fripp and myself in the present paper. This equation is for a straight line, the slope of which equals unity and is independent of the value of R. This does not agree with our experimental observations or with equation (3) derived by us in the paper. Furthermore, our reported results are for relatively small finite strains ($S \approx 0.7$); by contrast, equation (4) only holds for $S > 2.7$ ($\tanh S > 0.99$) which is equivalent to elongation strains > 15. Such large strains are not common in geological environments.

References

Bilby, B. A., Eshelby, J. D. & Kundu, A. K. 1975 *Tectonophysics* **28**, 265–274.
Cable, M. 1968 Proceedings of the VIIIth International Congress on glass, p. 163.
Gay, N. C. 1966 Unpublished Ph.D. thesis, University of London.
Gay, N. C. 1968 *Tectonophysics* **5**, 211–234.
Gay, N. C. 1969 *J. Geol.* **77**, 377–396.

PHILOSOPHICAL TRANSACTIONS OF THE ROYAL SOCIETY A MATHEMATICAL, PHYSICAL & ENGINEERING SCIENCES

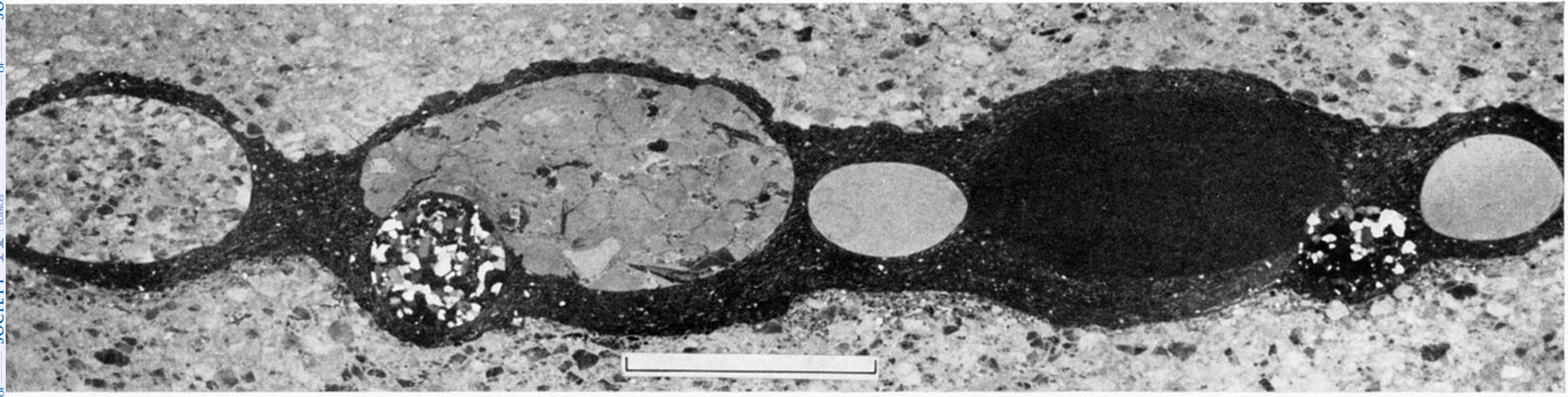

IGURE 4. An artificially deformed conglomerate: pebbles are (from left to right) Carrara marble; oolitic limestone and quartzite; Solenhofen limestone; shale; quartzite; and Solenhofen limestone. The pebbles are set in a matrix of mica schist and plaster of paris with an outer matrix of marble. (From Gay & Jaeger 1975.)

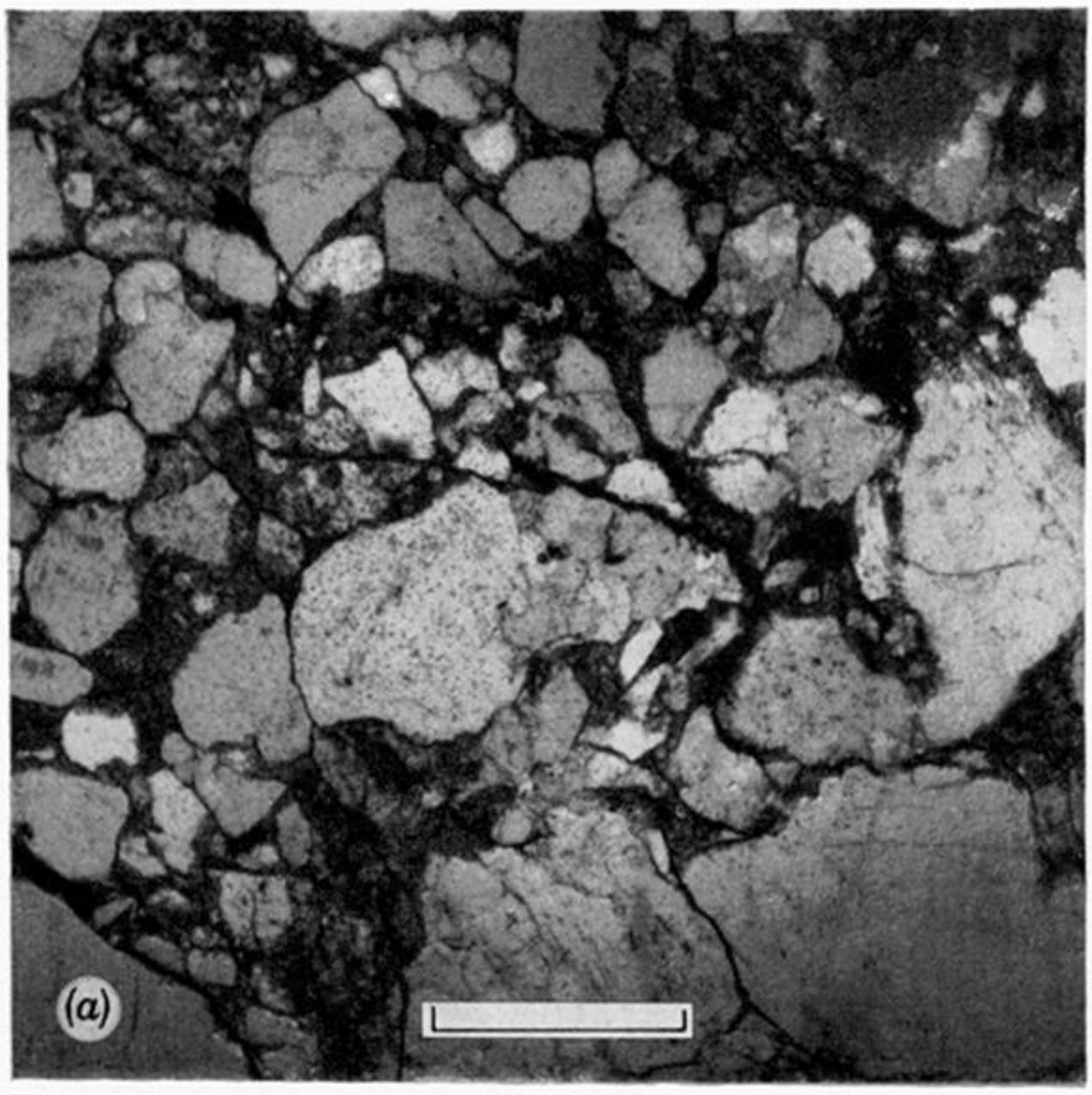

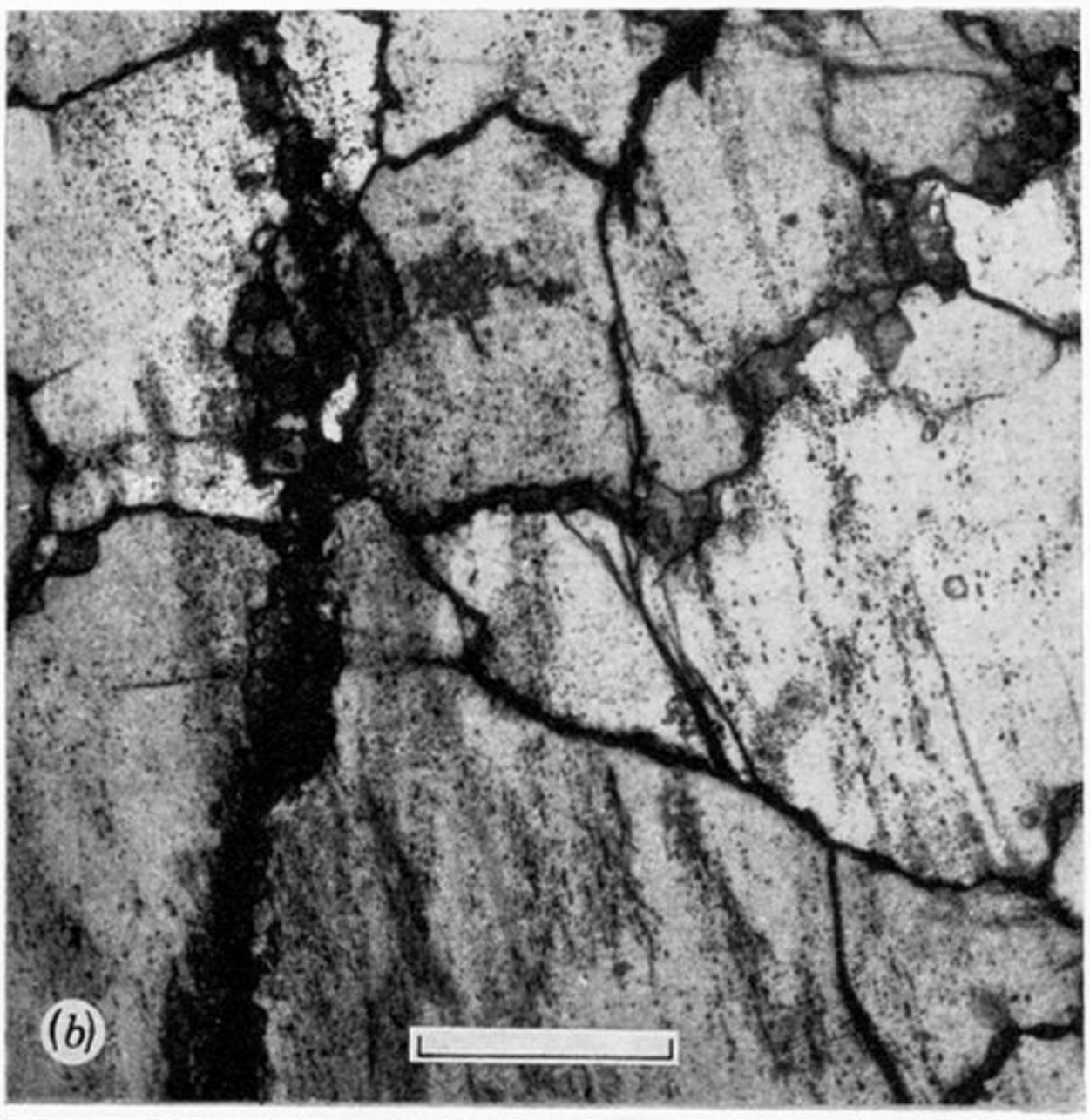

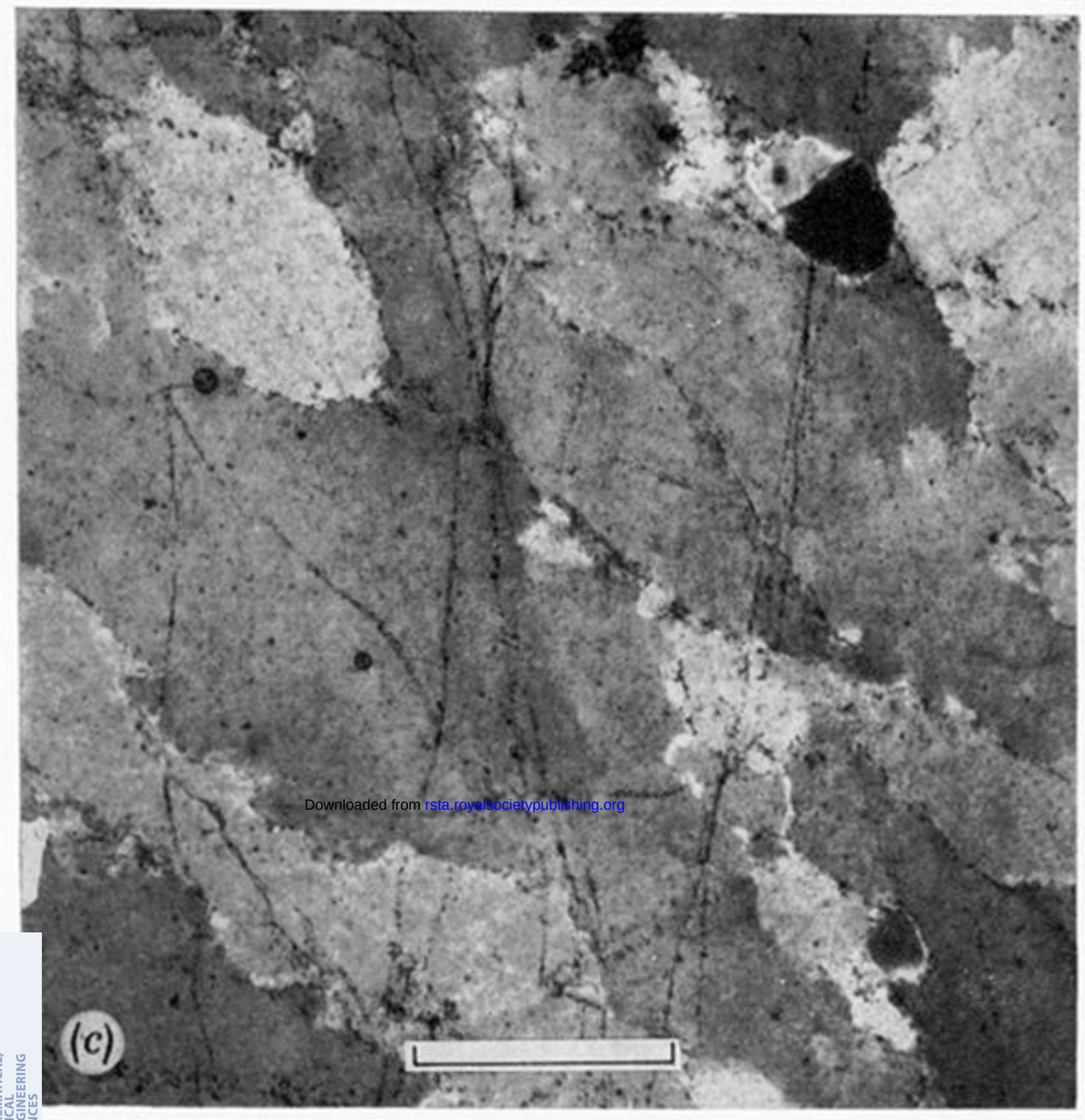

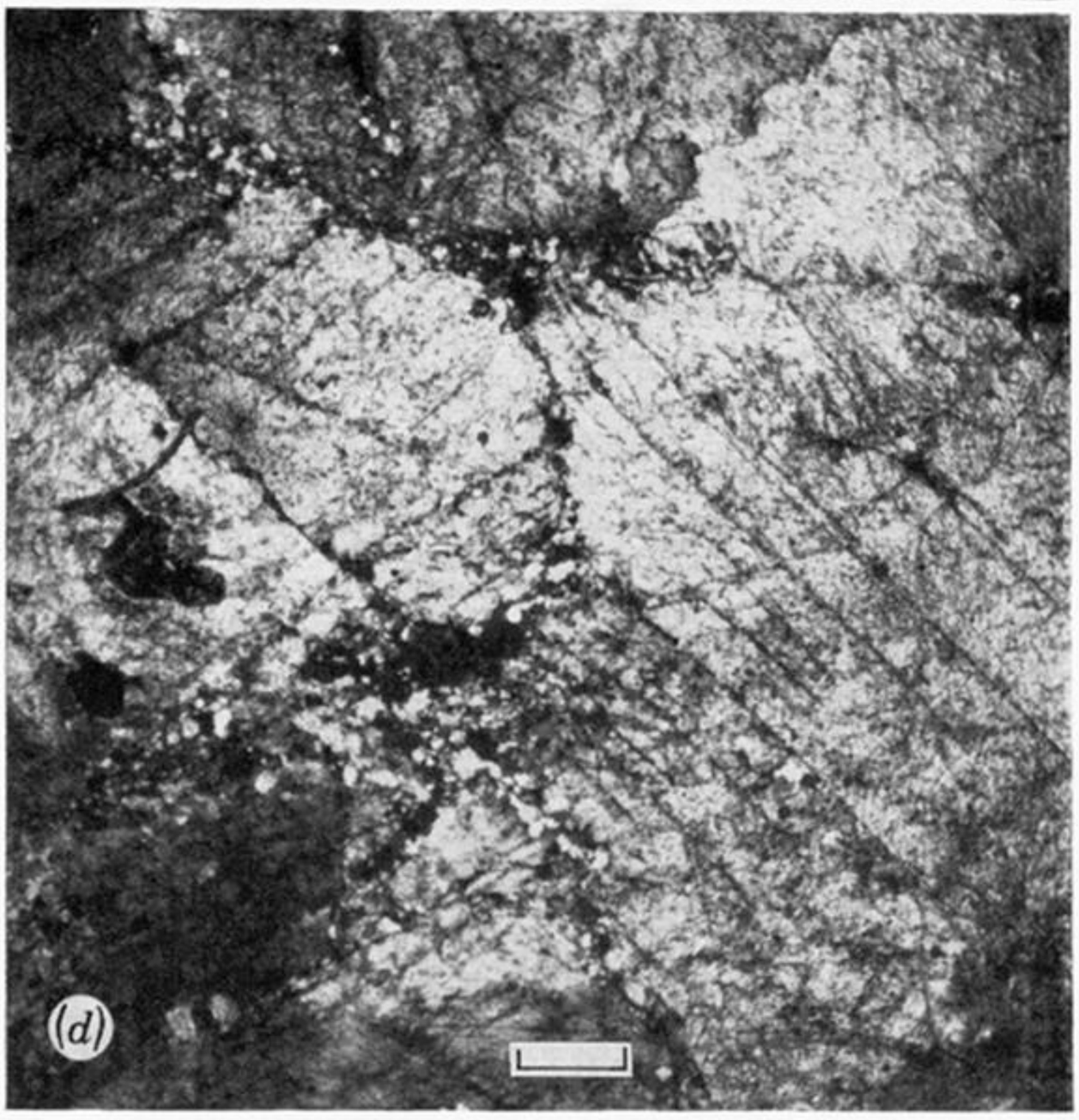

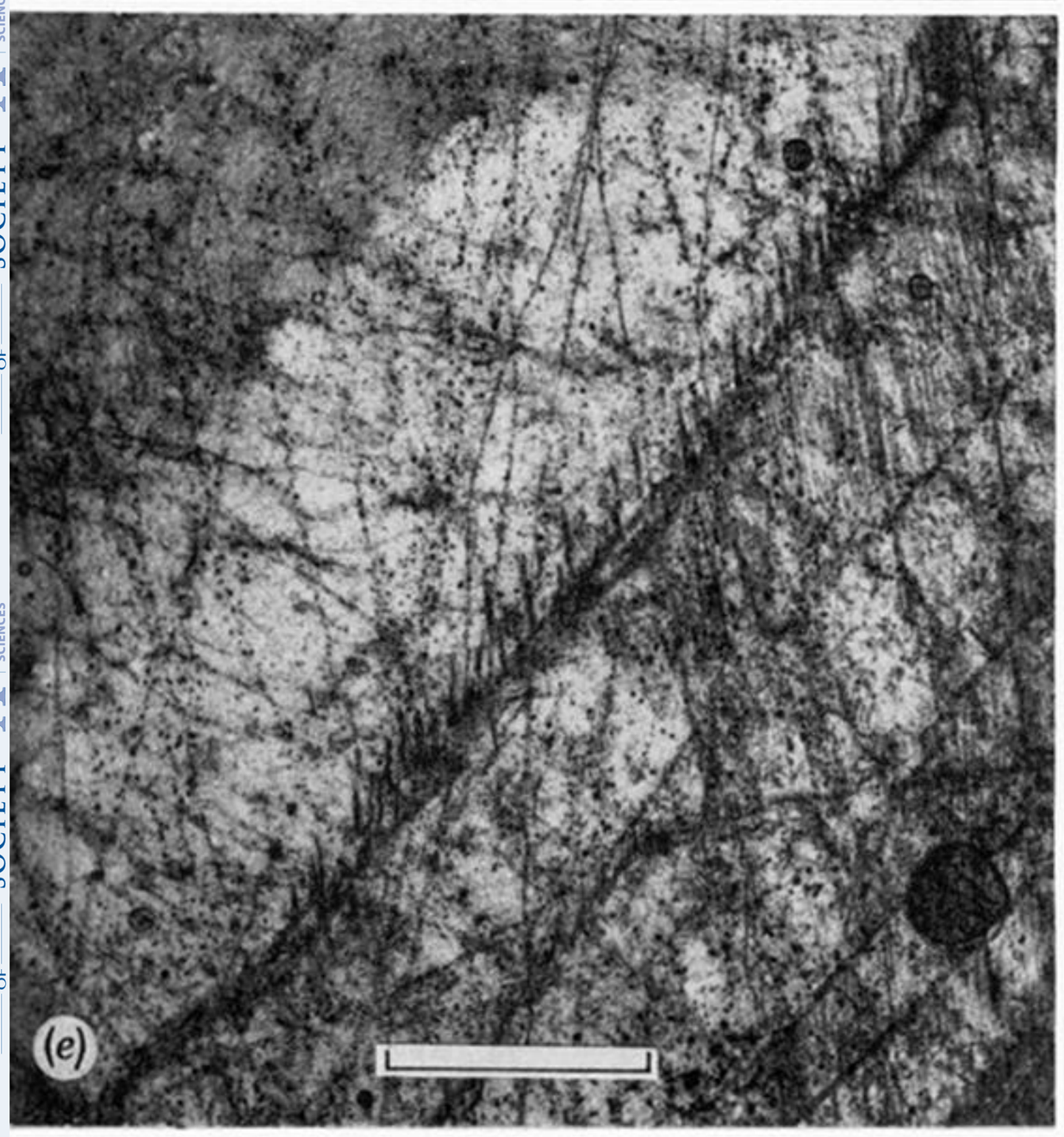

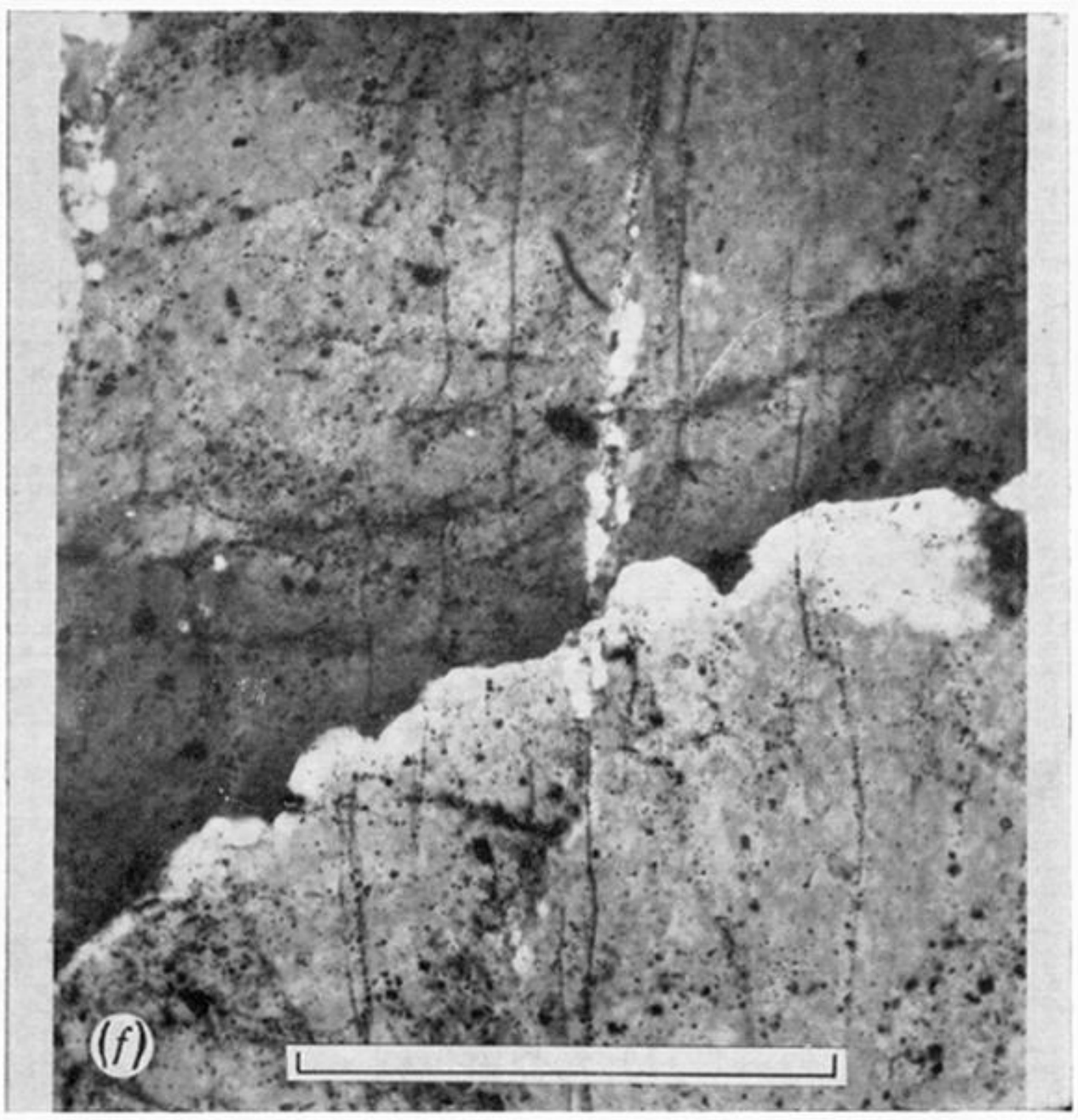

FIGURE 11. For description see opposite.